

Removal of Malachite Green Dye Using Oil Palm Empty Fruit Bunch as a Low-Cost Adsorbent

Rohani Mustapha ¹, Asmadi Ali ^{1,*}, Gunasangkari Subramaniam ¹, Anis Ayuni Aman Zuki ¹, Mohamad Awang ¹, Mohammad Hakim Che Harun ¹, Sofiah Hamzah ¹

¹ Environmental Sustainable Material Research Interest Group, Faculty of Ocean Engineering, Technology and Informatics, Universiti Malaysia Terengganu, 21030 Kuala Nerus, Terengganu Malaysia

* Correspondence: asmadi@umt.edu.my;

Scopus Author ID 54790692100

Received: 5.03.2021; Revised: 1.04.2021; Accepted: 3.04.2021; Published: 7.04.2021

Abstract: This present work is aimed to investigate the potential use of oil palm empty fruit bunch (EFB) as a low-cost adsorbent for the removal of malachite green dye. The untreated and treated palm oil empty fruit bunch characteristics were studied using Fourier Transform Infra-Red (FTIR) spectroscopy and scanning electron microscopy. The effects of initial concentration (20-100 mg/L) and adsorbent dosage (0.2-1.0 g) on the adsorption process were investigated to remove malachite green dye by batch adsorption method. Results show high-performance removal of dye for untreated and treated EFB with the adsorptive removal of 88.3% and 94.5% of the initial concentration and 80.84% and 88.07% of the adsorbent dosage. The adsorption isotherms were analyzed using Langmuir and Freundlich isotherm models. The results satisfactorily fitted with Langmuir isotherm revealed that monolayer adsorption mechanisms occurred on the EFB adsorbent surface. The maximum monolayer adsorption capacities were 714.3 mg/g and 1250 mg/g for untreated and treated EFB adsorbents, respectively. The overall results indicate that the treated EFB by alkaline method could be used as a promising low-cost adsorbent to remove the malachite green dye.

Keywords: oil palm empty fruit bunch; adsorbent; dye; isotherm.

© 2021 by the authors. This article is an open-access article distributed under the terms and conditions of the Creative Commons Attribution (CC BY) license (<https://creativecommons.org/licenses/by/4.0/>).

1. Introduction

The discharge of toxic colored effluent from the textile industry during the dyeing process is undeniable. About 10-15% of the dye from industries are directly discharged into the environment after the dyeing process, which may cause a negative impact on the ecosystem [1-3]. Malachite green (MG) dye is known as a hazardous dye for the environment and humans. MG is widely used for dyeing cotton, jute, silk, wool, and leather and used as a fungicide, anti-protozoan ectoparasites, and disinfectant in the fish farming industry [1, 4-6]. However, MG is linked to an increased risk of cancer, highly cytotoxic to mammalian cells, and acts as a liver tumor promoter [7-9]. Therefore, it is important to remove these dyes from industrial effluents before being discharged into the environment.

Numerous researchers discovered a variety of chemical, physical and biological treatment technologies to overcome dye contaminated water. Among all the available methods, the adsorption process is a preferred method due to its ease of operation, simplicity of design, high efficiency, and comparatively low cost of applying the decoloration process [10]. In the adsorption process, activated carbon is a commonly used adsorbent as it has excellent adsorption properties in removing different types of dyes and other toxic pollutants. However,

its application is limited due to its expensive cost [11]. Many efforts have focused on developing low-cost alternative adsorbents such as mineral, industrial by-products, and agricultural residues that are low cost and abundantly available [1, 12-14].

Empty fruit bunch (EFB) is an oil palm agricultural waste available in large quantities in Malaysia. About 1 ton of EFB solids were produced from each ton of oil extracted from the fruit bunch [15]. The EFB has no significant industrial and commercial uses, mostly dumped in landfills and pose severe environmental problems. Therefore, this study aims to explore the potential of untreated and alkaline treated empty fruit bunch (EFB) as an adsorbent for the removal of malachite green (MG) dye in an aqueous solution. The adsorbent characteristics and the effect on the parameters such as initial dye concentration and adsorbent dosage were investigated. The isotherm adsorption model was also studied.

2. Materials and Methods

2.1. Preparation of adsorbents and dye solution.

Empty fruit bunch (EFB) was obtained from Kilang Kelapa Sawit Sungai Tong at Setiu, Terengganu. The sample was cleaned with tap water several times to remove impurities and dust particles before it was washed with distilled water. The sample was dried in an oven at 105°C for 24 hours. The dried samples were manually cut into smaller sizes in the range of 0.5 to 1.0 cm and sieved to a size of 1 mm. The sieved sample was stored in an airtight plastic container and ready to be used as an untreated EFB. Meanwhile, treated EFB was prepared by adding the raw EFB into 0.1M of aqueous sodium hydroxide (NaOH) solution for 24 hours. Then the solution was decanted off, and the impregnated EFB was dried in the oven at 105°C overnight. The modified sample was rinsed with distilled water until the pH becomes neutral. The treated EFB was dried at 105°C for 24 hours. Finally, the treated EFB was cut into smaller sizes, same as untreated EFB before it was stored in the airtight container.

Malachite green dye, with chemical formula $C_{23}H_{25}ClN_2$, the molar mass of 364.911 g/mol, and λ_{max} of 617 nm, was purchased from Bendosen Laboratory Chemical. MG dye's molecular structure is illustrated in Figure 1. 1000 mg/L of MG dye stock solution was prepared by dissolving the dye's required amount in distilled water.

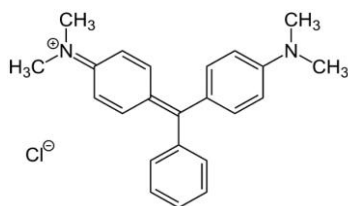


Figure 1. Structural formula of malachite green dye.

2.2. Characterization of adsorbents.

The EFB surface morphology was obtained by using JEOL JSM-6360LA scanning electron microscope (SEM) at the Scanning Electron Microscopy Unit Laboratory, Institute of Oceanography and Environmental, Universiti Malaysia Terengganu (UMT). The samples were mounted onto the SEM metal stub, followed by coating with a 20 nm thick layer of gold before viewing under the SEM. The surface morphology of untreated and treated EFB was compared. The surface functional group of adsorbents was determined by using Fourier Transform Infrared (FTIR) spectroscopy. The surface functional groups of untreated and treated EFB were analyzed in the range of 400-400 cm^{-1} . The surface charge of the adsorbents from EFB was

determined by using SurPASS electrokinetic analyzer. The adsorbents from EFB were loaded into the cylindrical cell before measuring the zeta potential by using the analyzer.

2.3. Batch adsorption studies

Batch adsorption experiments were conducted to evaluate the effects of initial dye concentration and adsorbent dosage. The experiment was carried out with 100 ml of dye solution in a 250 ml conical flask and agitated at 150 rpm in the water bath shaker at room temperature. The effect of initial dye concentration was carried out in the range of 20 to 100 mg/L at a constant adsorbent dosage of 0.2 g. Meanwhile, for the effect of adsorbent dosage, a range of adsorbent dosage from 0.2 to 1.0 g was used with 100 mg/L of initial dye concentration. The percentage of dye removal was calculated using the equation:

$$\% \text{ Dye removal} = [C_0 - C_i] / C_0 \times 100$$

where, C_0 is the initial dye concentration (mg/L) and C_i is the equilibrium dye concentration (mg/L).

3. Results and Discussion

3.1. Characterization of EFB adsorbents.

A scanning electron microscope was used to study the morphology of untreated and treated EFB. The SEM image of the surface morphology and cross-sectional of the untreated and treated EFB are shown in Figures 2(a) and 2(b), respectively. The pore space on the surface of untreated EFB is indistinctly visible and blocked by certain dirt particles and cementing substances.

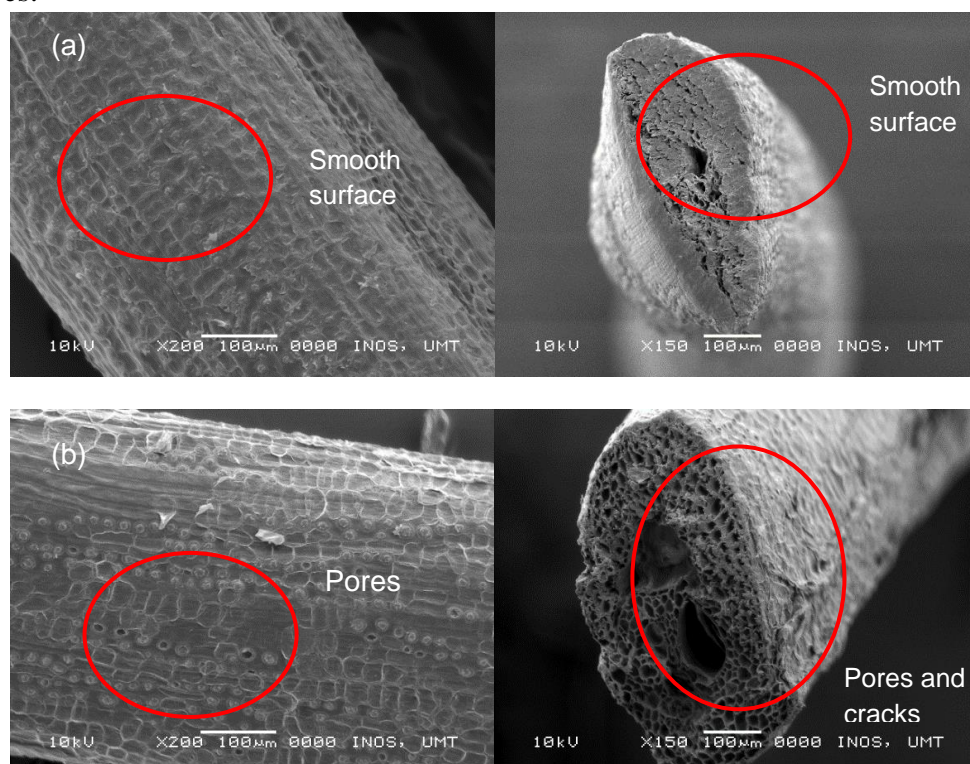


Figure 2. Surface morphology and cross-sectional of (a) untreated and (b) treated EFB adsorbent.

Besides that, the surface of untreated EFB shows a smooth and even surface due to the presence of lignin, hemicellulose, waxes, silica, and other dirt substances. The same

observations were reported by Chowdhury *et al.* [2] on the study of malachite green adsorption onto rice husk. Meanwhile, the surface of treated EFB is uneven, with many opened pore spaces. As reported by Naseer and their co-workers [16], the alkaline treated fiber was assisted in removing a certain quantity of the dirt substances and activated the hydroxyl groups of the EFB cellulose. Furthermore, the alkaline treatment of EFB has resulted in the changes to the structural linkage in the EFB feasibly through disruption of the hydrogen bonding and rearrangement of cellulose components through the formation of the new hydrogen bonds via intermolecular hydrogen bonding. This may lead to a higher dye adsorption capacity for treated EFB.

The FTIR spectra of untreated and treated EFB are presented in Figure 3. The broadband stretching at 3346 and 3343 cm^{-1} in the figure indicates O-H groups' presence due to the hydrogen bonding of polymeric compounds such as alcohols, phenols, and carboxylic in cellulose and lignin. The study of the methylene blue adsorption onto NaOH-treated coconut coir by Asim *et al.* [17] indicated that O-H groups' presence was shown the existence of 'free' hydroxyl groups on the adsorbent surface. The band at 2922 and 2920 cm^{-1} belongs to the C-H stretching vibration of aliphatic acids. This stretching indicates the presence of methyl and methylene groups in the EFB component [18]. The disappearance of the 1730 cm^{-1} band of the untreated EFB confirms the effectiveness of the alkaline treatment of EFB at removing a large portion of lignin and hemicellulose. This band basically represented the carbonyl functions of carboxylic acid, aldehyde, and ester groups peculiar to lignin. The same observation was showed by Djilali *et al.* [19] in the study of alkaline treated timber sawdust for removal of basic dyes. Meanwhile, the medium intensity peak at 1240 and 1249 cm^{-1} indicates the -C-O-C- β -glycosidic linkage in cellulose, and the sharp peak at 1031 cm^{-1} represents C-H in-plane deformation of lignin. The existence of β -glycosidic linkage is due to the presence of lignin in lignocellulose material. Those functional groups' intensity for treated EFB was lower than untreated EFB confirmed that treated EFB has a lower amount of lignin. According to Chakraborty *et al.* [20], the lignin existence can minimize the binding of available functional groups on the adsorbent surface and adsorbate molecules.

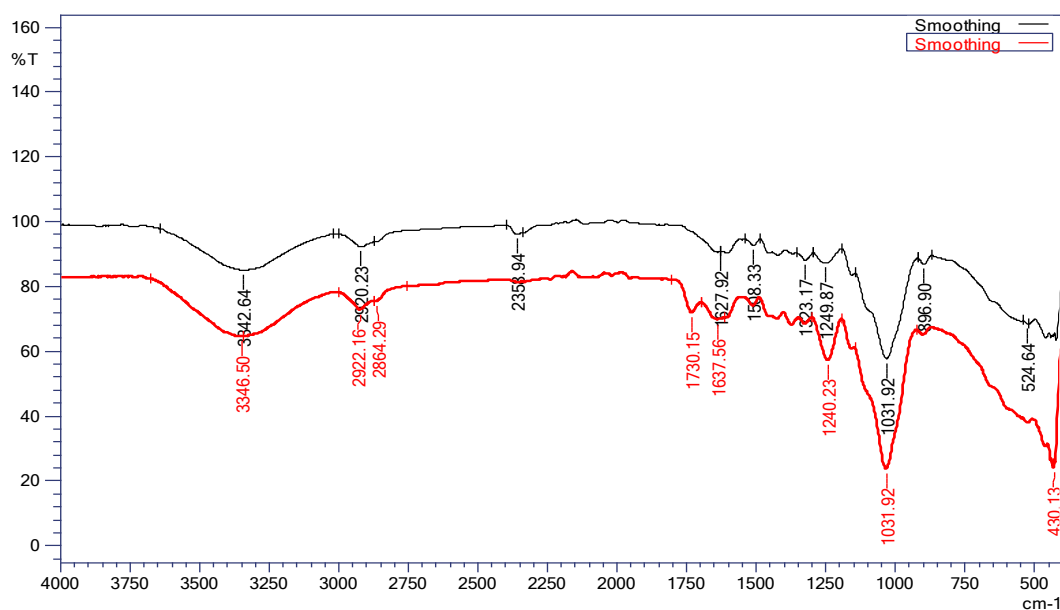


Figure 3. FTIR spectrum of untreated and treated EFB adsorbent.

Table 1 shows the comparison of the BET surface area and total pore volume of EFB adsorbents with other adsorbents from previous studies by other researchers. The BET surface

area of untreated and treated EFB were 0.95 and 0.63 m²/g, respectively. Meanwhile, the total pore volume of untreated and treated EFB were 0.002 and 0.0013 cm³/g, respectively. The BET surface area for both EFB adsorbents was almost similar to the BET surface area of wheat shells adsorbents. The adsorbent's surface area's low value was due to the difficulties involved in degassing the lignocellulosic samples because the powder is burnt even before reaching the degassing temperature. Thus, the degassing temperature (100°C) is reduced, resulting in a low surface area due to moisture [21].

Table 1. Comparison of the BET surface area and total pore volume of EFB adsorbents with some other studies.

Adsorbent	BET surface area, m ² /g	Total pore volume, cm ³ /g	References
Untreated EFB	0.95	0.0020	This study
Treated EFB	0.63	0.0013	This study
Peanut shell	2.2	-	Herbert <i>et al.</i> [22]
Rice straw carbon	1.16	0.0028	Saad <i>et al.</i> [23]
Wheat shells	0.67	-	Bulut and Aydin [24]
Banana peels	0.65	-	Pathak and Mandavgane [21]
Foumanat tea waste	45.0	-	Ebrahimian <i>et al.</i> [18]
Flax Seed Ash Beads	45.01	0.041	Işık and Uğraşkan [12]
Green pea peels	316.20	0.2717	Dod <i>et al.</i> [25]
Cashew nut shell	395.00	0.4732	Senthil Kumar <i>et al.</i> [26]
Pumpkin seeds	737.90	0.3700	Njoku <i>et al.</i> [27]

Surface charges of EFB adsorbents were obtained from the zeta potential by using an electrokinetic analyzer (EKA). The surface charges of adsorbents were important to know the adsorbent surface's principle and its surrounding interactions. Table 2 shows the zeta potential of untreated and treated EFB were recorded from -21.180 to -24.936 and -27.505 to -30.208 mV, respectively. According to Li *et al.* [28], this negative surface charge of lignocellulosic materials is associated with carboxyl and phenolic OH groups. The charge on the surface of treated EFB was more negative than that of untreated EFB leaves, suggesting that alkali treatment onto the adsorbents enhances OH ions' negative charge on the surface adsorbents. Similar results were reported in the study of adsorbent from bark which is from -13.9 to -31.6 mV [29].

Table 2. Zeta potential of untreated and treated EFB adsorbents.

Ramp	Zeta potential (mV)	
	Untreated EFB	Treated EFB
1	-22.257	-29.990
2	-22.024	-28.510
3	-21.180	-27.505
4	-24.936	-30.208

3.2. Batch adsorption studies.

3.2.1. Effect of initial dye concentration.

The percentage of MG dye removal for untreated and treated EFB, as shown in Figures 4(a) and (b), increased from 80.6 to 88.3% and 88.1 to 94.5% with the decrease in the initial dye concentration from 20 to 100 mg/L, respectively. The higher percentage dye removal is obtained at a lower concentration as there is less MG quantity to be adsorbed at a lower concentration than high concentration Maia *et al.* [30]. There is no reduction in removal capacity of treated EFB, unlike untreated EFB. These results clearly proved that the alkaline treatment of EFB effective in removing MG dye due to their rough surface and the existence of the 'free' hydroxyl groups on the adsorbent surface. The uptake of MG dye increased with the increase in contact time. The equilibrium removal of MG was obtained after 480 min contact time. The initial adsorption was rapid at first 30 min, and after that, it proceeded at a

slower rate (30-420min) and finally reached equilibrium. The findings are due to the initial concentration increases, and the mass transfer driving force becomes higher, hence resulting in larger MG adsorption. The same findings were reported by Nasrullah *et al.* [31] on the study of methylene blue adsorption on various carbon.

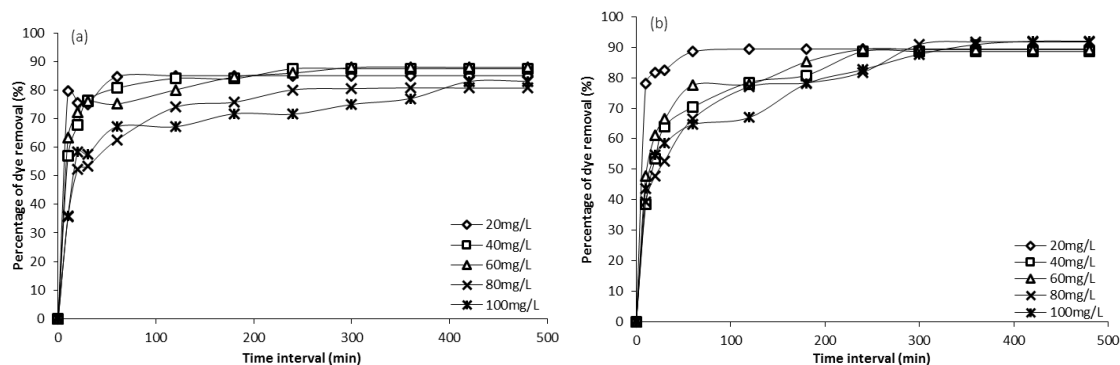


Figure 4. Effect of initial dye concentration on dye adsorption onto (a) untreated and (b) treated EFB adsorbents.

3.2.2. Effect of adsorbent dosage.

Figure 5(a) and (b) show the effect of adsorbent dosage on the MG dye removal onto untreated and treated EFB, respectively. MG dye's uptake onto untreated EFB increased from 57.34 to 80.84% when the adsorbent dosage increases from 0.2 to 0.8g and then reduces to 79.36% at 1.0g adsorbent dosage. However, the percentage of dye removal for treated EFB increased from 79.13 to 88.07% with the increase of adsorbent dosage from 0.1 to 1.0g. The increase was due to the higher MG dye molecules were attached to the adsorbent surface site and thus reduce the repulsion between the solute molecules of the solid and bulk phases [32]. The removal of MG dye for treated EFB was higher than untreated EFB due to the alkaline treatment of adsorbent that offered more pores to the surface of adsorbent than the untreated EFB.

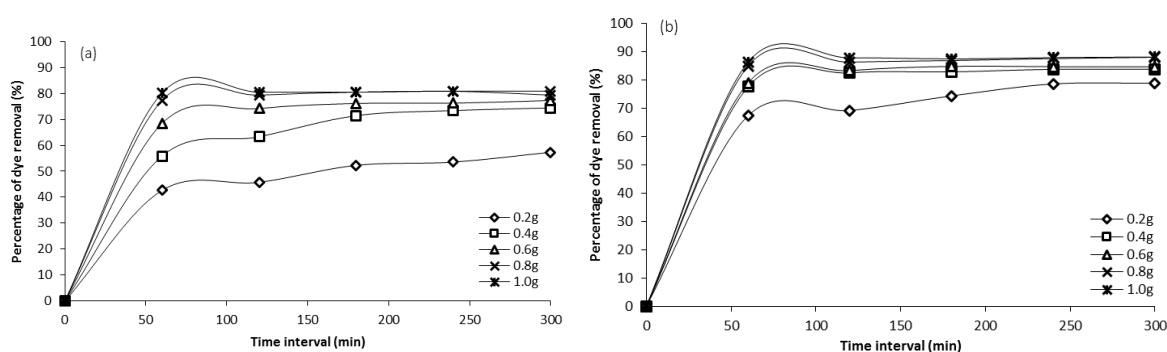


Figure 5. Effect of adsorbent dosage on dye adsorption onto (a) untreated and (b) treated EFB adsorbents.

3.2.3. Adsorption isotherm.

The adsorption isotherm is mainly significant in describing how solutes interact with adsorbents and is important in enhancing adsorbents [1]. The obtained results from the equilibrium conditions were studied based on Langmuir and Freundlich adsorption isotherms. The Langmuir isotherm assumes monolayer adsorption onto a surface containing a finite number of adsorption sites of uniform approaches with no shifting of adsorbate in the plane surface [33]. The Langmuir adsorption isotherm model is depicted in the equation:

$$1/q_e = 1/(q_{\max} \cdot K_L \cdot C_e) + 1/q_{\max}$$

where q_e is the amount of dye adsorbed at equilibrium (mg/g), C_e is the MG dye concentration (mg/L), q_{\max} is the maximum monolayer adsorption capacity of the adsorbent (mg/g), and K_L is the Langmuir adsorption constant related to the free energy adsorption (L/mg). The linear plots of specific adsorption ($1/q_e$) against the equilibrium concentration ($1/C_e$) for dye adsorption onto untreated and treated EFB are shown in Figure 6. The isotherm constants, K_L , and equilibrium monolayer capacities, q_{\max} can be evaluated from the intercept and the plots' slope. The Langmuir parameters are listed in Table 3. The R^2 values show that the adsorption isotherms fit the Langmuir isotherm with the correlation coefficient of 0.9455 and 0.9888 for the adsorption of MG dye onto untreated and treated EFB, respectively.

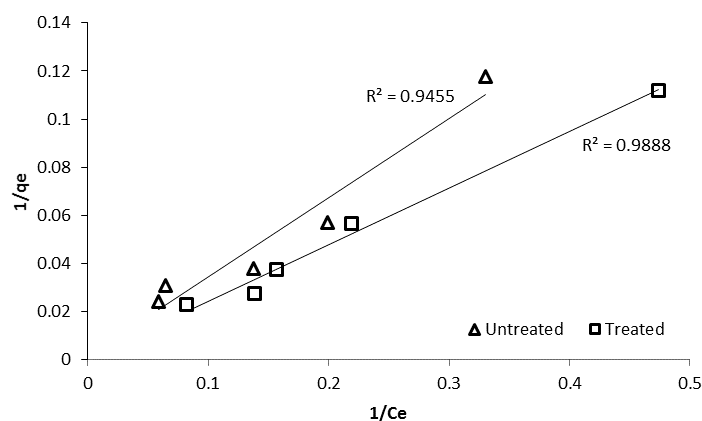


Figure 6. Langmuir isotherms.

The essential characteristics of the Langmuir isotherm can be expressed in terms of a dimensionless constant separation factor R_L that is given in equation:

$$R_L = 1 / (1 + (C_0 \cdot K_L))$$

where C_0 is the highest initial MG dye concentration (mg/L). The value of R_L shows the shape of the isotherm to be either unfavourable ($R_L > 1$), linear ($R_L = 1$), favourable ($0 < R_L < 1$), or irreversible ($R_L = 0$). The value of R_L was found to be 0.702 and 0.746 for the untreated and treated EFB, respectively, thus confirms that both adsorbents from EFB favor the adsorption of MG dye. Furthermore, the q_{\max} values of the adsorption of MG dye on the treated EFB were higher than the value of the untreated EFB, which are 1250 and 714.3 mg/g, respectively. Based on Table 4, the values of q_{\max} for EFB adsorbents were almost similar to other adsorbents from previous studies by other researchers.

Table 3. Parameters of adsorption isotherm of untreated and treated EFB adsorbents.

Adsorbent	Untreated EFB	Treated EFB
<i>Langmuir isotherm</i>		
q_{\max} (mg/g)	714.3	1250.0
K_L (L/mg)	0.0043	0.0034
R_L	0.702	0.746
R^2	0.9455	0.9888
<i>Freundlich isotherm</i>		
$K_F(\text{mg/g}(\text{L/mg})^{1/n})$	4.212	1.4494
$1/n$	0.807	0.546
R^2	0.9107	0.9449

The adsorption isotherm was further studied by using the Freundlich isotherm model. The Freundlich isotherm is commonly used to describe the adsorption characteristics for the heterogeneous surface [34]. The Freundlich model is depicted in the equation:

$$\log q_e = \log K_F + \log C_e (1/n)$$

where, K_F is the Freundlich constant (mg/g.mg), and n is a constant related to the adsorption intensity. Both constants are obtained from the plot's interception and slope, respectively. From the plot of $\log q_e$ against $\log C_e$ as shown in Figure 7, the correlation coefficient R^2 for the adsorption of MG dye onto untreated and treated EFB are 0.9107 and 0.9449, respectively.

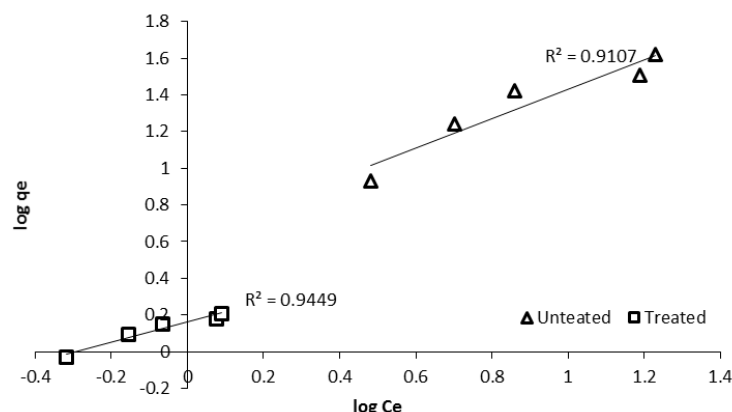


Figure 7. Freundlich isotherms.

Table 4. Comparison of maximum adsorption capacity of EFB adsorbents with other adsorbents.

Adsorbent	Dye	Max. adsorption capacity, q_{max} (mg/g)	References
Untreated EFB	Malachite green	714.3	This study
Treated EFB	Malachite green	1250.0	This study
Bark	Basic red 2	1119.0	McKay <i>et al.</i> [35]
Rice husk	Basic red 2	838.0	McKay <i>et al.</i> [35]
Tree fern	Basic red 13	408.0	Ho <i>et al.</i> [36]
Cottonseed hull	Neutral red	166.7	Zhou <i>et al.</i> [37]
Palm kernel shell	Methylene blue	183.4	García <i>et al.</i> [38]
<i>C. equisetifolia</i> needle	Methylene blue	110.8	Dahri <i>et al.</i> [39]
<i>C. equisetifolia</i> needle	Malachite green	77.6	Dahri <i>et al.</i> [39]
Potato plant waste	Malachite green	27.0	Gupta <i>et al.</i> [40]

4. Conclusions

The present study shows that treated EFB is an effective adsorbent for removing MG in the aqueous solution. The surface morphology and functional group of treated EFB were enhancing the higher adsorption of MG dye. The parameters such as initial dye concentration and adsorbent dosage were found to affect the adsorption efficiency of treated EFB with the higher percentage of MG dye removal. The MG dye adsorption onto EFB followed Langmuir isotherm model with the maximum adsorption capacity of 714.3 mg/g and 1250 mg/g.

Funding

This research received no funding.

Acknowledgments

The authors are grateful to Universiti Malaysia Terengganu for providing facilities for this study.

Conflicts of Interest

The authors declare no conflict of interest.

References

1. Karayunlu Bozbas, S.; Karabulut, M. Reusing menengic (*Pistacia terebinthus*) coffee waste as an adsorbent for dye removal from aqueous solution. *International Journal of Environmental Analytical Chemistry* **2021**, *00*, 1–19. <https://doi.org/10.1080/03067319.2021.1873312>.
2. Chowdhury, S.; Mishra, R.; Saha, P.; Kushwaha, P. Adsorption thermodynamics, kinetics and isosteric heat of adsorption of malachite green onto chemically modified rice husk. *Desalination* **2011**, *265*, 159–168. <http://dx.doi.org/10.1016/j.desal.2010.07.047>.
3. Pavani, K. V.; Srujana, N.; Preethi, G.; Swati, T. Immobilization of lignin peroxidase from *Alcaligenes aquatilis* and its application in dye decolorization. *Letters in Applied NanoBioScience* **2020**, *2*, 1058–1063. <https://doi.org/10.33263/LIANBS92.10581063>.
4. Mohamad, M.; Wannahari, R.; Mohammad, R.; Shoparwe, N. F.; Nawi, A. S. M.; Lun, K. W.; Wei, L. J. Adsorption of malachite green dye using spent coffee ground biochar: optimisation using response surface methodology. *Jurnal Teknologi* **2020**, *83*, 28–36. <https://doi.org/10.11113/jurnalteknologi.v83.14904>.
5. Gong, R.; Jin, Y.; Chen, F.; Chen, J.; Liu, Z. Enhanced malachite green removal from aqueous solution by citric acid modified rice straw. *Journal of Hazardous Materials* **2006**, *137*, 865–870. <http://dx.doi.org/10.1016/j.jhazmat.2006.03.010>.
6. Meinertz, J.; Stehly, G.; Gingerich, W.; Allen, J. Residues of [¹⁴C]-malachite green in eggs and fry of rainbow trout, *Oncorhynchus mykiss* (Walbaum), after treatment of eggs. *J Fish Diseases* **1995**, *18*, 239–248. <http://dx.doi.org/10.1111/j.1365-2761.1995.tb00299.x>.
7. Zadvarzi, S. B.; Khavarpour, M.; Vahdat, S. M.; Baghbanian, S. M.; Rad, A. S. Synthesis of Fe₃O₄@chitosan@ZIF-8 towards removal of malachite green from aqueous solution: Theoretical and experimental studies. *International Journal of Biological Macromolecules* **2021**, *168*, 428–441. <https://doi.org/10.1016/j.ijbiomac.2020.12.067>.
8. Panandiker, A.; Fernandes, C.; Gundu Rao, T.; Kesava Rao, K. Morphological transformation of Syrian hamster embryo cells in primary culture by malachite green correlates well with the evidence for formation of reactive free radicals. *Cancer Letters* **1993**, *74*, 31–36. [http://dx.doi.org/10.1016/0304-3835\(93\)90040-g](http://dx.doi.org/10.1016/0304-3835(93)90040-g).
9. Rizk, N. M. H.; Eldourghamy, A. S.; Aly, S. A.; Sabae, S. Z.; Sobhy, A. Production of Lignin Peroxidase from Aquatic Bacteria, *Alcaligenes aquatilis* Nashua. *Egyptian Journal of Aquatic Biology and Fisheries* **2020**, *24*, 213–223. <https://doi.org/10.21608/ejabf.2020.90301>.
10. Zaghoul, A.; Abali, M.; Ichou, A. A.; Benhiti, R.; Soudani, A. Adsorption of Anionic Dyes Using Monoionic and Binary Systems: a Comparative Study. *Letters in Applied NanoBioScience* **2021**, *10*, 2588–2593. <https://doi.org/10.33263/LIANBS103.25882593>.
11. Bello, O. S.; Alao, O. C.; Alagbada, T. C.; Agboola, O. S.; Omotoba, O. T.; Abikoye, O. R. A renewable, sustainable and low-cost adsorbent for ibuprofen removal. *Water Science and Technology* **2021**, *83*, 111–122. <https://doi.org/10.2166/wst.2020.551>.
12. Işık, B.; Uğraşkan, V. Adsorption of methylene blue on sodium alginate–flax seed ash beads: Isotherm, kinetic and thermodynamic studies. *International Journal of Biological Macromolecules* **2021**, *167*, 1156–1167. <https://doi.org/10.1016/j.ijbiomac.2020.11.070>.
13. Putri, K. N. A.; Kaewpichai, S.; Keereerak, A.; Chinpa, W. Facile Green Preparation of Lignocellulosic Biosorbent from Lemongrass Leaf for Cationic Dye Adsorption. *Journal of Polymers and the Environment* **2021**. <https://doi.org/10.1007/s10924-020-02001-5>.
14. Tang, X.; Ran, G.; Li, J.; Zhang, Z.; Xiang, C. Extremely efficient and rapidly adsorb methylene blue using porous adsorbent prepared from waste paper: Kinetics and equilibrium studies. *Journal of Hazardous Materials* **2021**, *402*, 123579. <https://doi.org/10.1016/j.jhazmat.2020.123579>.
15. Chang, S. H. An overview of empty fruit bunch from oil palm as feedstock for bio-oil production. *Biomass and Bioenergy* **2014**, *62*, 174–181. <https://doi.org/10.1016/j.biombioe.2014.01.002>.
16. Naseer, R.; Afzal, N.; Zulfikar-Ul, H.; Saeed, S.; Mujahid, H.; Faryal, S.; Aslam, S.; Habib-Ur, R. Effect of bronsted base on topological alteration of rice husk as an efficient adsorbent comparative to rice husk ash for azo dyes. *Polish Journal of Environmental Studies* **2020**, *29*, 2795–2802. <https://doi.org/10.15244/pjoes/112353>.
17. Asim, N.; Amin, M. H.; Alghoul, M. A.; Sulaiman, S. N. A.; Razali, H.; Akhtaruzzaman, M.; Amin, N.; Sopian, K. Developing of Chemically Treated Waste Biomass Adsorbent for Dye Removal. *Journal of Natural Fibers* **2019**, *00*, 1–10. <https://doi.org/10.1080/15440478.2019.1675214>.

18. Ebrahimian Pirbazari, A.; Saberikhah, E.; Badrouh, M.; Emami, M. S. Alkali treated Foumanat tea waste as an efficient adsorbent for methylene blue adsorption from aqueous solution. *Water Resources and Industry* **2014**, *6*, 64–80. <http://doi.org/10.1016/j.wri.2014.07.003>.
19. Djilali, Y.; Elandalousi, E. H.; Aziz, A.; de Ménorval, L.-C. Alkaline treatment of timber sawdust: A straightforward route toward effective low-cost adsorbent for the enhanced removal of basic dyes from aqueous solutions. *Journal of Saudi Chemical Society* **2012**, *20*, S241-S249. <http://doi.org/10.1016/j.jscs.2012.10.013>.
20. Chakraborty, S.; Chowdhury, S.; Das Saha, P. Adsorption of Crystal Violet from aqueous solution onto NaOH-modified rice husk. *Carbohydrate Polymers* **2011**, *86*, 1533–1541. <http://doi.org/10.1016/j.carbpol.2011.06.058>.
21. Pathak, P. D.; Mandavgane, S. A. Preparation and characterization of raw and carbon from banana peel by microwave activation : Application in citric acid adsorption. *Journal of Environmental Chemical Engineering* **2015**, *3*, 2435–2447. <http://doi.org/10.1016/j.jece.2015.08.023>.
22. Herbert, A.; Kumar, U.; Janardhan, P. Removal of hazardous dye from aqueous media using low-cost peanut (*Arachis hypogaea*) shells as adsorbents. *Water Environment Research* **2020**, 0–3. <https://doi.org/10.1002/wer.1491>.
23. Saad, M. J.; Sajab, M. S.; Busu, W. N. W.; Misran, S.; Zakaria, S.; Chin, S. X.; Chia, C. H. Comparative adsorption mechanism of rice straw activated carbon activated with NaOH and KOH. *Sains Malaysiana* **2020**, *49*, 2721–2734. <https://doi.org/10.17576/jsm-2020-4911-11>.
24. Bulut, Y.; Aydın, H. A kinetics and thermodynamics study of methylene blue adsorption on wheat shells. *Desalination* **2006**, *194*, 259–267. <http://doi.org/10.1016/j.desal.2005.10.032>.
25. Dod, R.; Banerjee, G.; Saini, S. Adsorption of methylene blue using green pea peels (*Pisum sativum*): A cost-effective option for dye-based wastewater treatment. *Biotechnology and Bioprocess Engineering* **2012**, *17*, 862–874. <http://doi.org/10.1007/s12257-011-0614-5>.
26. Senthil Kumar, P.; Ramalingam, S.; Senthamarai, C.; Niranjanaa, M.; Vijayalakshmi, P.; Sivanesan, S. Adsorption of dye from aqueous solution by cashew nut shell: Studies on equilibrium isotherm, kinetics and thermodynamics of interactions. *Desalination* **2010**, *261*, 52–60. <http://doi.org/10.1016/j.desal.2010.05.032>.
27. Njoku, V. O.; Foo, K. Y.; Hameed, B. H. Microwave-assisted preparation of pumpkin seed hull activated carbon and its application for the adsorptive removal of 2,4-dichlorophenoxyacetic acid. *Chemical Engineering Journal* **2013**, *215-216*, 383–388. <http://doi.org/10.1016/j.cej.2012.10.068>.
28. Li, J.; Li, H.; Yuan, Z.; Fang, J.; Chang, L.; Zhang, H.; Li, C. Role of sulfonation in lignin-based material for adsorption removal of cationic dyes. *International Journal of Biological Macromolecules* **2019**, *135*, 1171–1181. <https://doi.org/10.1016/j.ijbiomac.2019.06.024>.
29. Argun, M. E.; Dursun, S.; Karatas, M. Removal of Cd(II), Pb(II), Cu(II) and Ni(II) from water using modified pine bark. *Desalination* **2009**, *249*, 519–527. <http://doi.org/10.1016/j.desal.2009.01.020>.
30. Maia, L. S.; da Silva, A. I. C.; Carneiro, E. S.; Monticelli, F. M.; Pinhati, F. R.; Mulinari, D. R. Activated Carbon From Palm Fibres Used as an Adsorbent for Methylene Blue Removal. *Journal of Polymers and the Environment* **2020**, *29*, 1162-1175. <https://doi.org/10.1007/s10924-020-01951-0>.
31. Nasrullah, A.; Bhat, A. H.; Naeem, A.; Isa, M. H.; Danish, M. High surface area mesoporous activated carbon-alginate beads for efficient removal of methylene blue. *International Journal of Biological Macromolecules* **2018**, *107*, 1792–1799. <https://doi.org/10.1016/j.ijbiomac.2017.10.045>.
32. Salleh, M. A. M.; Mahmoud, D. K.; Karim, W. A.; Idris, A. Cationic and anionic dye adsorption by agricultural solid wastes: A comprehensive review. *Desalination* **2011**, *280*, 1–13. <https://doi.org/10.1016/j.desal.2011.07.019>.
33. Foo, K.Y.; Hameed, B.H. Insights into the modelling of adsorption isotherm systems, *Chemical Engineering Journal* **2010**, *156*, 2–10. <https://doi.org/10.1016/j.cej.2009.09.013>.
34. Kocaman, S. Removal of methylene blue dye from aqueous solutions by adsorption on levulinic acid-modified natural shells. *International Journal of Phytoremediation* **2020**, *22*, 885–895. <https://doi.org/10.1080/15226514.2020.1736512>.
35. McKay, G.; Porter, J. F.; Prasad, G. R. The removal of dye colors from aqueous solution by adsorption on low-cost materials. *Water Air Soil Pollution* **1999**, *114*, 423–438. <https://doi.org/10.1023/A:1005197308228>.
36. Ho, Y.S.; Chiang, T.H.; Hsueh, Y.M. Removal of basic dye from aqueous solution using tree fern as a biosorbent, *Process Biochem.* **2005**, *40*, 119–124. <https://doi.org/10.1016/j.procbio.2003.11.035>.

37. Zhou, Q.; Gong, W.; Xie, C.; Yang, D.; Ling, X.; Yuan, X.; Chen, S.; Liu, X. Removal of neutral red from aqueous solution by adsorption on spent cottonseed hull substrate. *Journal of Hazardous Materials* **2011**, *185*, 502–506. <http://doi.org/10.1016/j.jhazmat.2010.09.029>.
38. García, J. R.; Sedran, U.; Zaini, M. A. A.; Zakaria, Z. A. Preparation, characterization, and dye removal study of activated carbon prepared from palm kernel shell. *Environmental Science and Pollution Research* **2018**, *25*, 5076–5085. <https://doi.org/10.1007/s11356-017-8975-8>.
39. Dahri, M. K.; Raziq, M.; Kooh, R.; Lim, L. B. L. Application of Casuarina equisetifolia needle for the removal of methylene blue and malachite green dyes from aqueous solution. *Alexandria Engineering Journal* **2015**, *54*, 1253–1263. <http://doi.org/10.1016/j.aej.2015.07.005>.
40. Gupta, N.; Kushwaha, A. K.; Chattopadhyaya, M. C. Application of potato (*Solanum tuberosum*) plant wastes for the removal of methylene blue and malachite green dye from aqueous solution. *Arabian Journal of Chemistry* **2011**, *9*, S707–S716. <http://doi.org/10.1016/j.arabjc.2011.07.021>.